DOI: 10.1002/ejic.200700416

Silicon–Phosphorus and Silicon–Arsenic Cage Compounds with Bicyclo[2.2.1]heptane, Bicyclo[3.2.1]octane and Tricyclo[3.3.3.1.0^{3,7}]nonane Backbones

Günter Tekautz,[a] Judith Baumgartner,[a] Alk Dransfeld,[a] and Karl Hassler*[a]

Keywords: Cage compounds / Crystal structures / Ab initio calculations / Silicon

The reaction of tris(chlorodimethylsilyl)methylsilane (**1**) and 1,1,2,2-tetrakis(chlorodimethylsilyl)-1,2-dimethyldisilane (**2**) with sodium/potassium arsenide Na_3As/K_3As afforded decamethyl-2,3,5,6,7-pentasila-1,4-diarsabicyclo[2.2.1]heptane (**3**) and dodecamethyl-2,3,4,6,7,8,9-heptasila-1,5-diarsatricyclo-[3.3.1.0^{3,7}]nonane (**4**). Compounds **3** and **4** were isolated from the reaction mixture by fractional crystallization and structurally characterized by single-crystal X-ray crystallography. The reaction of **1** with an excess amount of sodium/potassium phosphide (Na_3P/K_3P) afforded the cage-shaped anion sodium hexamethyl-2,4,6,7-tetrasila-1-phosphanido-3,5-diphosphabicyclo[3.2.1]octane (**5**), which reacts with chlorotrimethylsilane to form trimethylsilyl-substituted derivative **6**. The molecular structures of **5** and **6** were established by X-ray crystallography. Cages **3**–**6** were also characterized by ^{29}Si- and ^{31}P NMR spectroscopy. Owing to indirect spin–spin coupling between the ^{29}Si and ^{31}P nuclei, the resonances of the ^{29}Si nuclei in the spectra of **5** and **6** are only of first order approximately. To account for the observed preferences of the cage structures in these reactions, extensive B3LYP/6-31G* quantum chemical calculations of relative energies of bicyclo[2.2.2] and bicyclo[3.2.1] isomers of Si_8H_{14}, PSi_7H_{13}, $P_2Si_6H_{12}$ and $P_3Si_5H_{11}$ were conducted. On the basis of the computed charge distributions, the concept of topological charge stabilization was used to predict the relative stabilities.

Introduction

The exceptional tendency of the elements silicon (group 14) and phosphorus (group 15) to form rings and cages is well-known and has been reviewed extensively in the past.[1] Much less experimental and theoretical material is available for the heavier elements of these two groups, which are Ge, Sn and Pb and As, Sb and Bi, respectively. As the metallic character of the elements increases with increasing atomic number, the thermal stability of E_nR_m (where R is an organic substituent, for example) decreases considerably. They easily decompose into the metal, thereby forming R–R bonds, as shown in Equation (1). Flasks with metallic-black coatings are a common sight with this type of chemistry.

$$E_nR_m \rightarrow E_{metal} + m/2\ (R_2) \quad (1)$$

It is clear that rings and cages composed of elements of both group 14 and 15 (for instance Si and P, As, Sb or Bi) will behave similarly in this respect. An important difference, however, is in the polar bonds that are present in these cage compounds as a result of the electronegativity difference between the two elements. Not only does this lead to increased chemical reactivity, but also to interesting electronic effects. For instance, in small ring systems such as 1,3-disiladiphosphabicyclobutanes, the ring-strain energy is considerably increased by the electropositive Si atoms, which is reflected in a unusually large P–P distance of 238 pm.[2] Moreover, cage compounds that are composed of elements from group 15 and silicon that also possess Si–Si bonds show unusual electronic interactions between the lone pairs of electrons of the group 15 element and the Si–Si σ electrons. A n→σ* interaction was shown by NBO ab initio calculations and photoelectron spectra of dodecamethyl-2,3,5,6,7,8-hexasila-1,4-diphosphabicyclo[2.2.2]-octane to be responsible for these interactions. X-ray analysis of the molecular structure confirmed the increased Si–Si bond length in the cage, which is reported as 235.9 and 236.3 pm.[3,4] Normal Si–Si bond lengths are 232–234 pm.

Previously, we have reported on the synthesis and molecular structure of decamethyl-2,3,5,6,7-pentasila-1,4-dibismuthabicyclo[2.2.1]heptane from Na_3Bi/K_3Bi and dichlorodimethylsilane,[5] which decomposes quickly at room temperature forming metallic bismuth. We also reported the synthesis and structure of decamethyl-2,3,5,6,7-pentasila-1,4-diphosphabicyclo[2.2.1]heptane from Na_3P/K_3P and 1,2-dichlorotetramethyldisilane.[4] These syntheses show that in the reactions between sodium/potassium pnictides and halogenated mono- and oligosilanes, Si–Si bonds are not only cleaved, but new bonds are formed depending on

[a] Institute of Inorganic Chemistry, University of Technology, Stremayrgasse 16, 8010 Graz, Austria
E-mail: günter.tekautz@tugraz.at
baumgartner@tugraz.at
alk.dransfeld@tugraz.at
karl.hassler@tugraz.at

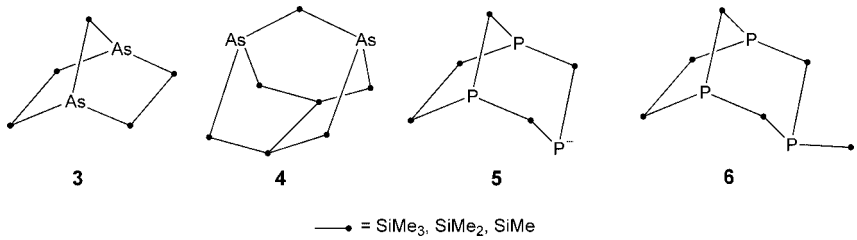

Figure 1. Cage compounds prepared in this work.

the reaction conditions. This was also reported for the reaction of tBuSi($SiMe_2Cl$)$_3$ with $LiPH_2$, which resulted in the formation of a hexasila-1,5-diphosphabicyclo[3.2.1]octane.[6]

These findings prompted us to not only use halogenated isotetrasilanes but larger oligosilanes as well to form novel cage compounds. Moreover, by varying the stoichiometric ratio between the halosilane and the sodium/potassium pnictide, we expected the formation of novel anionic species with cage-like structures. We were pleased to learn that this is indeed possible. Herein we report the synthesis of hitherto unknown silicon–arsenic cages **3** and **4** as well as anionic silicon–phosphorus cage **5** and its trimethylsilyl derivative **6** as shown in Figure 1 starting from the oligosilanes MeSi($SiMe_2Cl$)$_3$ (**1**) and ($SiMe_2Cl$)$_2$MeSiSiMe($SiMe_2Cl$)$_2$ (**2**) and Na_xP/K_xP or Na_xAs/K_xAs.

Results and Discussion

Synthesis

As mentioned in the introduction, the products formed in the reactions between sodium/potassium pnictides and multiply halogenated oligosilanes depend strongly on the reaction conditions, and the largest influence comes from the solvent that is used. In polar solvents such as dimethoxyethane (dme), Si–Si bonds of the oligosilane are broken and reformed to a certain extent to give -E$SiMe_2$E- and even -EMe_2Si$SiMe_2$E atom arrangements when MeSi($SiMe_2Cl$)$_3$ is used. Even traces of ($SiMe_2$)$_6$ can be detected in the reaction mixtures with ^{29}Si NMR spectroscopy. Of course, considerable quantities of polymers are also formed in these reactions. Whereas insoluble polymers are removed in the workup process, the soluble fraction may severely hamper successful crystallization of the cage compounds. We also found that the quantities of polymers that are formed are much larger for arsenic compounds than for phosphorus compounds, which we attribute to the much greater reducing power of sodium/potassium arsenide. So far, no systematic experimental studies on the influence of the solvent and the pnictogen/alkali metal ratio on the product distribution of these reactions have been described.

The mechanisms of these reactions are not known. The formation of silylenoide species $Me_2SiNaCl$ or dimethylsilylene, $SiMe_2$, as intermediates through Si–Si bond cleavage seems plausible. For instance, the formation of such species is thought to play a major role during the reduction of dichlorodimethylsilane with alkali metals.[7]

The silylenes can then insert into Si–Si, Si–P, Si–As or Si–Cl bonds to give a plethora of compounds. When Na_3As/K_3As reacts with **1** at r.t., cage **3** can be isolated in about 5% yield. We did not attempt to optimize the reaction conditions. Cage **3** is not the only cage that forms under these conditions, because in the ^{29}Si NMR spectrum of the reaction mixture we observed, besides the signal of hexasila-1,4-diarsabicyclo[2.2.2]octane, three resonances at –70.0, –17.1 and 5.0 ppm, which we attribute to an adamantane-like structure, as shown in Figure 2. So far, we were unable to purify this compound by crystallization. In this molecule, the Si_4 atom arrangement of **1** is still present.

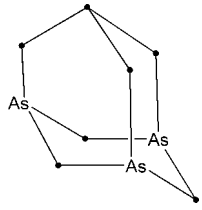

Figure 2. Proposed structure for adamantane $As_3Si_7Me_{13}$.

When Na_3As/K_3As reacts with **2**, tricyclononane **4** forms in about 5% yield and can be separated by crystallization. Here again we performed no optimization of the reaction conditions. From the ^{29}Si NMR spectra it can be concluded that there are other cage compounds present in the reaction mixture, such as bicycloheptane **3**, which can be identified unambiguously. So far, all attempts to isolate other cage compounds by fractional crystallization have failed.

Noteworthy is that the tricyclononane structure established for **5** by X-ray diffraction can also be found as P_9 groups (alternating with P_8 groups) in Hittorf's violet monoclinic phosphorus allotrope, as shown in Figure 3.[8] Recently, the crystal structure of a fibrous variation of violet phosphorus, which also contains the P_8 and P_9 units, was reported.[9] For us, the P_2Si_7 cage (analogous to **4**) and the

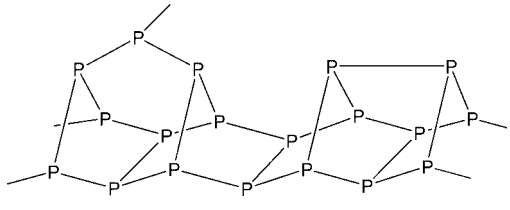

Figure 3. P_9 and P_8 substructures in violet phosphorus and in its fibrous variation.

tricyclooctanes E_2Si_6 (E = As, P) analogous to P_8 are tempting synthetic targets that we are currently pursuing by reaction of **2** with Na_3E/K_3E under various conditions.

When a suspension of an excess amount of Na_3P/K_3P in dme is added to a solution of **1** in dme heated at reflux, anionic cage **5** can be separated by crystallization from pentane/dme. As a byproduct, decamethyl-2,3,5,6,7-pentasila-1,4-diphosphabicyclo[2.2.1]heptane is formed in considerable quantities.

X-ray Crystallography

Crystals of cages **3**, **4**, **5** and **6** in a quality suitable for X-ray experiments could be obtained as described in the Experimental Section. Figure 4 presents the molecular structures of these compounds, and Table 1 summarizes selected bond lengths and bond angles by employing the numbering scheme of Figure 4. The molecular symmetry of all four molecules is C_s, characterized by a mirror plane bisecting the cages.

The Si–As and Si–P bond lengths are all within the expected range found in acyclic silylphosphanes and their arsenic analogues. Si–Si distances are longer than the normal 232–234 pm by about 30 pm for P cages **5** and **6**, and by about 10 pm for arsenic cage **3**, which reflects the decreasing n→σ* interaction of arsenic relative to phosphorus. The Si(2)–Si(3) bond length in **4** is in the normal range because just one As atom is available for this interaction. The central Si–Si bond in **4** is somewhat longer (235.2 pm), which certainly is due to steric reasons.

Table 1. Selected bond lengths [pm] and bond angles [°] for **3**, **4**, **5** and **6**.

	3	**4**	**5**	**6**
Si(1)–E(1)	236.73(9)	237.19(16)	224.83(30)	226.25(11)
Si(2)–E(1)	236.46(9)	236.24(18)	225.00(30)	227.09(11)
Si(3)–P(1)			228.45(30)	226.03(13)
Si(3)–P(2)			218.70(20)	226.05(13)
Si(4)–P(2)				226.57(13)
Si(2)–Si(2′)	235.53(10)		236.35(20)	237.50(11)
Si(2)–Si(3)		233.80(20)		
Si(3)–Si(3′)		235.20(20)		
E(1)–Si(1)–E(1′)	111.07(3)	126.74(7)	114.59(10)	114.11(4)
E(1)–Si(2)–Si(2′)	109.10(3)		108.39(9)	108.24(4)
As(1)–Si(2)–Si(3)		105.38(7)		
Si(2)–Si(3)–Si(3′)		103.80(8)		
Si(1)–E(1)–Si(2)	92.12(3)	102.33(6)	93.93(9)	95.17(4)
Si(1)–P(1)–Si(3)			103.39(9)	104.13(4)
Si(2)–As(1)–Si(2′′)	101.38(3)	94.46(6)		
Si(2)–P(1)–Si(3)			103.16(9)	103.40(4)
Si(4)–P(2)–Si(3)				106.35(4)
Si(3)–P(2)–Si(3′)				105.78(4)
C–Si(1)–C	106.86(14)	106.40(30)	104.42(4)	105.81(13)

NMR Spectra

Because of the quadrupole moment of the ^{75}As nucleus, the ^{29}Si NMR spectra of **3** and **4** are simple and consist of

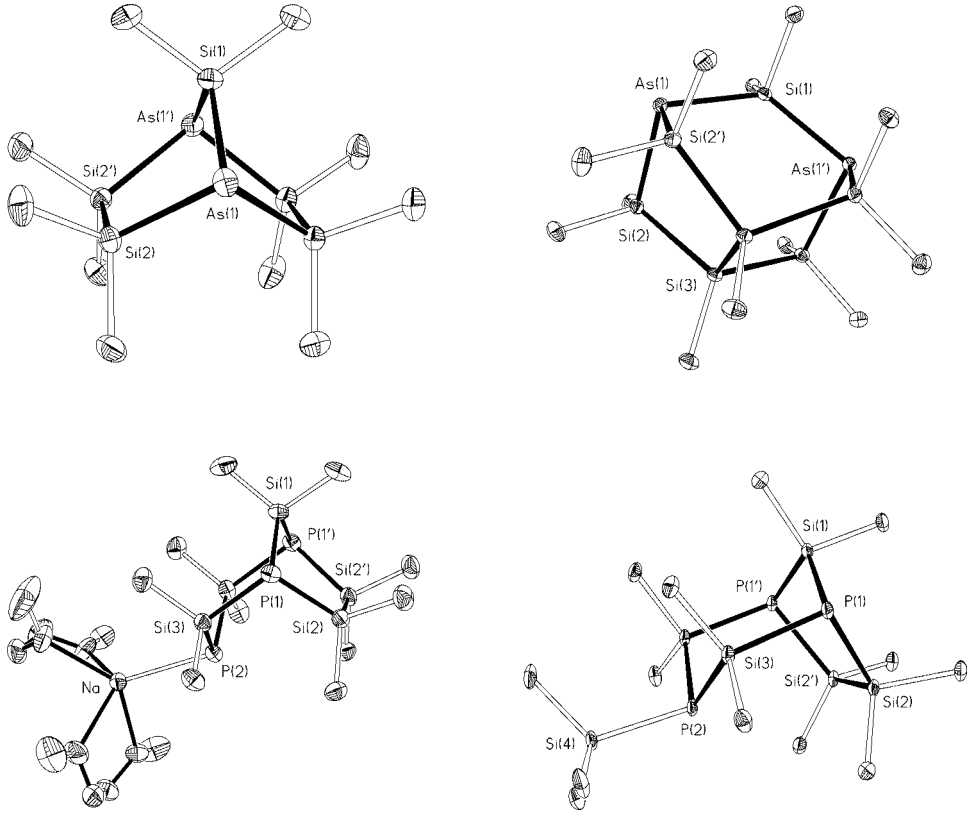

Figure 4. ORTEP plots (30% probabilities) of the molecular structures for **3** (top, left), **4** (top, right), **5** (bottom, left) and **6** (bottom, right).

Table 2. Chemical shifts [ppm, $\delta(^{29}Si)$ against TMS, $\delta(^{31}P)$ against 85% H_3PO_4] and coupling constants [Hz] for cages **3**, **4**, **5** and **6**.

	3	**4**	**5**				**6**			
	δ	δ	δ	J			δ	J		
				P1	P1′	P2		P1	P1′	P2
Si(1)	26.6	–1.7	17.1	50.9	50.9	0	13.9	47.9	47.9	0
Si(2)	1.2	–3.2	–4.2	39.5	6.2	0	–4.7	40.5	4.8	3.0
Si(3)		–73.8	4.9	39.7	0	81.4	1.3	46.4	0	49.5
Si(4)							2.4	0	0	39.8
P(1)			–247.1			2.1	–238.9			8.3
P(2)			–261.9				–231.0			

just two signals for **3** and three signals for **4**. Table 2 summarizes the $\delta(^{29}Si)$ values with reference to the atom numbers that are used in Figure 4.

The spectra of phosphorus cages **5** and **6** are different, as not all signals are necessarily of first order as a result of indirect spin–spin coupling between the ^{29}Si and ^{31}P nuclei. For instance, Si(2) is part of an ABX system with $\delta(A) \approx \delta(B)$ because the shift differences between P(1) and P(1′) is due to isotopic effects only. The ABX system itself is weakly coupled to phosphorus atom P(2). From spectra simulations with various fixed values for $^2J_{P1,P1'}$ it is quickly deduced that this coupling constant must be quite small (<2–4 Hz), and that the spectra can be evaluated by using first-order rules to a very good accuracy. The g NMR software package was used for this purpose.

Figure 5 presents the measured ^{29}Si NMR spectra of **5** (top left) and **6** (top right), as well as the simulated spectra. The spectrum of **5** consists of a triplet of doublets for Si(1) at +17ppm, a doublet of doublets for Si(3) at +5 ppm and doublet of doublets of doublets for Si(3) at –4 ppm. The spectrum for **6** is very similar except that the resonance for Si(4) (the $SiMe_3$ group) overlaps the multiplet of Si(3). A view of the expanded spectrum for **6** is given at the bottom of Figure 5 and illustrates the effects of two- or three-bond couplings. All chemical shifts and coupling constants, treating all spectra as first order, are presented in Table 2.

The Si,P coupling constants of **5** and **6** are very similar, except between Si(3) and P(2). In anionic cage **5**, a J value of 81.4 Hz was measured, but this value was only 49.5 Hz in cage **6** where the negative charge is replaced by the trimethylsilyl group. Bond lengths P(2)–Si(3), which are 218.7 and 226.1 pm, respectively (Table 1), are also quite different. A shortening of the Si–P bonds by 6–10 pm upon substitution of a $SiMe_3$ group with a negative charge is also observed for $P(SiMe_3)_3$ and the phosphanides $MP(SiMe_3)_2$, M = K, Rb and Cs.[10,11]

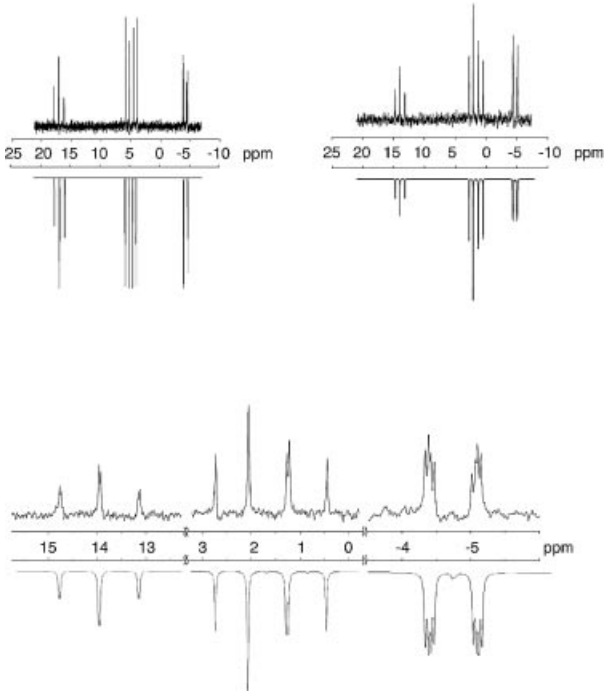

Figure 5. Proton decoupled ^{29}Si NMR spectra of **5** (top left) and **6** (top right), including simulated spectra shown with negative intensities. An expanded spectrum of **6** is presented at the bottom and illustrates the splitting due to two- and three-bond $^{29}Si,^{31}P$ couplings.

Ab Initio Calculations

The number of different anionic species that are present in the "Zintl phases" prepared from the elements P or As and sodium/potassium alloy in a solvent such as dme is unknown. Most certainly, not all P–P or As–As bonds are broken in this reaction, and an equilibrium between the various anions is established depending on the stoichiometric ratio of phosphorus/alkaline metals used. For instance, $(Me_3Si)_2PP(SiMe_3)_2$ and $P_7(SiMe_3)_3$ are just two minor by-products in the synthesis of $P(SiMe_3)_3$ from "Na_3P/K_3P" and Me_3SiCl. An even larger variety of Si_mP_n frameworks can be formed when Si–Si bonds in reagents **1** and **2** are broken under the attack by "Na_3P/K_3P". Because only a few of the potential species are observed, the question arises whether the obtained product distribution can be deduced from simple considerations. Cages such as diphosphabicyclo[2.2.1]heptanes and diphosphabicyclo[2.2.2]octanes are prevalent in the reaction mixtures, whereas triphosphabicyclo[2.2.2]octanes A or B shown in Scheme 1 do not form at all in the reaction with $Me_2SiClSiClMe_2$ or Me_2SiCl_2.

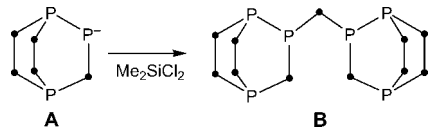

Scheme 1. Cages that are not formed.

Because the major products obtained experimentally comprise eight second-row atoms, the computational study focuses on bicyclic Si_8, PSi_7, P_2Si_6 and P_3Si_5 structures. Our approach to rationalize the observations is the concept of topological charge stabilization advocated by Gimarc 20 years ago.[12] It predicts that by replacing a silicon atom in one of the Si_nP_m cages by an atom of higher electronegativity, P, at the site with the highest electron density leads to the most stable isomer.

We first calculated minimum structures, energies and Mulliken charges for the isomeric Si_8H_{14} structures. The five lowest-energy isomers are shown in Figure 6 together with the Mulliken charge of the Si atom possessing the highest electron density. Replacing it by P should result in the best PSi_7H_{13} structure. Only the two best homonuclear frameworks, the bicyclo[2.2.2] and bicyclo[3.2.1] cages that differ by just 0.9 kJ mol^{-1}, are considered in the further replacement study.[13] With a value of about 40 kJ mol^{-1}, the relative energies of the bicyclo[4.2.0] and bicyclo[4.1.1] structures are large. The bicyclo[5.1.0] cage has an even higher energy of 117 kJ mol^{-1}. These large values can be used to rationalize why we never observed their formation.

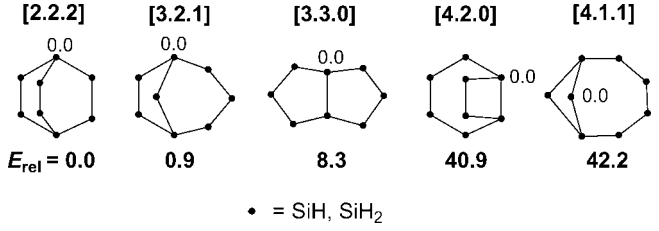

Figure 6. Relative energies [kJ mol^{-1}] of bicyclic Si_8H_{14} isomers and the position of the Si atom possessing the smallest Mulliken charge. Relative energies are given for the most favourable stereoisomer or conformer. A dot represents a SiH_2 or SiH group.

As shown in Figure 7 (1st row), the relative energies of the two bicyclo[2.2.2] and the three bicyclo[3.2.1] topomers of PSi_5H_{13} demonstrate the validity of the Gimarc rule. The Mulliken charges (the position with the smallest value is indicated in Figure 7) predict that the diphospha[2.2.2] and diphospha[3.2.1] cages with P atoms in 1,4- and 1,5-positions will be preferred, which is just what we observed in numerous experiments. In the second row of Figure 7, the relative energies of the two sets of $P_2Si_6H_{12}$ topomers are presented, again confirming the predictions of the Gimarc rules.

Although the bicyclo[2.2.2] structure is higher in energy than bicyclo[3.2.1] by 6.7 kJ mol^{-1}, both are considered in the final replacement for obtaining the energies of the triphospha cages. The results are summarized in the third row of Figure 7. The charge distribution in bicyclo[2.2.2] $P_2Si_6H_{12}$ clearly suggests that the 1,2,4-triphospha isomer will be preferred. Consequently, its energy relative to the 1,2,3- and 1,2,6-triphospha isomer is predicted to be lower by more than 45 kJ mol^{-1}. The situation is less clear for the bicyclo[3.2.1] framework, because in the lowest energy isomer the two smallest atomic charges differ by merely 0.01 units. According to Gimarc's rule, the 1,3,5- and the 1,5,8-

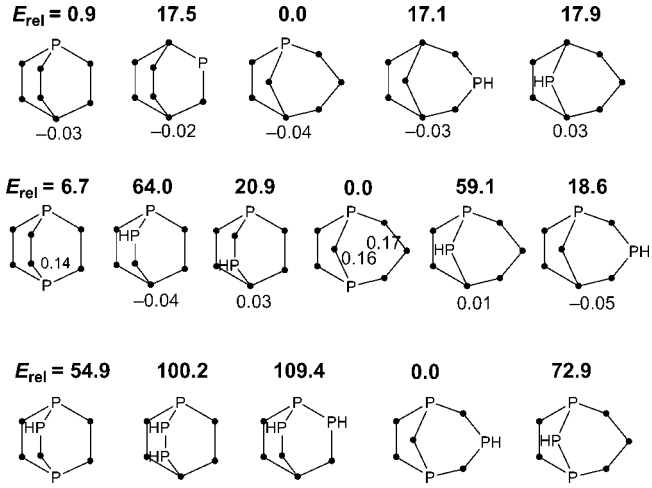

Figure 7. Relative energies [kJ mol^{-1}] of the bicyclic PSi_7H_{13}, $P_2Si_6H_{12}$ and $P_3Si_5H_{11}$ isomers, and the position of the Si atom possessing the smallest Mulliken charge. Relative energies are given for the most favourable stereoisomer or conformer.

isomer are predicted to possess very similar energies, and both should be present in the reaction mixture. Nevertheless, the charges in the second best structure indicate that the 1,3,5-P_3Si_5 backbone is preferred. The calculated relative energy of 72.9 kJ mol^{-1} for the 1,5,8-structure provides clear preference for 1,3,5-isomer, which is what we found in the experiment.

Our ab initio calculations indicate that isomers with P–P bonds generally have higher energies. This agrees with the lack of observation of these isomers in the synthesis. Owing to $^{31}P,^{31}P$ one bond coupling, their presence would have been detected very easily by using NMR spectroscopy.

The general conclusion that the polar Si–P bond is favoured over the nonpolar Si–Si as well as the P–P bond was quantified by the comparative calculation of two saturated $P_2Si_2H_8$ isomers. $H_3Si–SiH_2–PH–PH_2$ has a relative energy of 32.8 kJ mol^{-1} with respect to $H_3Si–PH–SiH_2–PH_2$, which both have the same number of Si–H and P–H bonds. In conclusion, the Si–P bond is favoured by about 16 kJ mol^{-1} over a Si–Si or a P–P bond in phosphasilanes. Analysis of all investigated cage isomers deposited at nmr-sharc.tugraz.at shows that the relative energies are positively related to the $(n_{SiSi} + n_{PP})/n_{SiP}$ ratio, where n_{SiSi}, n_{PP} and n_{SiP} are the number of Si–Si, P–P and Si–P bonds, respectively. Therefore, it can be generalized that cage isomers with a maximum number of Si–P bonds will be energetically preferred.

Conclusions

In the present publication we showed that by reaction of sodium/potassium phosphide and arsenide with chlorooligosilanes containing $SiMe_2Cl$ end groups, anionic and neutral cage compounds containing E–$SiMe_2$–E and E–$SiMe_2$–$SiMe_2$–E atom arrangements can be obtained. A plausible reaction mechanism explaining Si–Si bond cleavage involves dimethylsilylene as a reaction intermediate. In that case, a donor interaction with a P atom on the surface of the solid

must be assumed. Noteworthy, chlorodisilanes disproportionate by such a donor mechanism in the presence of amines, even in heterogeneous phase.[14]

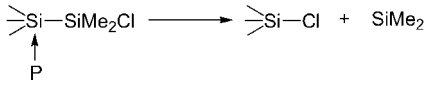

The preferred formation of 1,4-diphosphahexasilabicyclo[2.2.2]octanes and 1,3,5-triphosphapentasilabicyclo-[3.2.1]octanes over other topological isomers could be rationalized by using the concept of topological charge stabilization.

Experimental Section

General: All experiments were performed under anaerobic conditions by using standard Schlenk techniques. Solvents were dried with sodium or potassium and distilled under an atmosphere of N_2 prior to use. Starting materials **1** and **2** were prepared as described in the literature. ^{31}P and ^{29}Si NMR spectra were recorded with a BRUKER MSL 300 spectrometer (59.627 MHz for ^{29}Si, 121.451 MHz for ^{31}P). Chemical shifts are given in ppm relative to 85% aq. H_3PO_4 for ^{31}P and $SiMe_4$ for ^{29}Si (external). Elemental analyses were performed with a HERAEUS VARIO EL. As compounds **3**–**5** are extremely sensitive towards traces of oxygen and moisture, the quality of the elemental analyses is not as good as usually achieved.

Decamethyl-2,3,5,6,7-pentasila-1,4-diarsabicyclo[2.2.1]heptane (3): To a suspension of "Na_xAs/K_xAs" [prepared from Na (1.10 g, 48.22 mmol), K (1.50 g, 38.58 mmol) and As (5.0 g, 74.92 mmol) by a modified procedure described by Becker[15]] in dme (300 mL) was added dropwise a solution of **1** (9.37 g, 28.9 mmol) in dme (70 mL) over a period of 60 min. During the reaction, which is exothermic, the black colour of the suspension changed to yellow-green. The reaction mixture was then heated at reflux for 8 h, and the precipitated salts were separated by filtration. The solvent was then removed by evaporation in vacuo and replaced by heptane. Subsequently, the solution was decanted from the remaining salts, and **3** (1.7 g, 5%) was obtained by fractional crystallization at –30 °C. $C_{10}H_{30}As_2Si_5$ (440.62): calcd. C 27.26, H 6.86; found C 28.57, H 7.28.

Dodecamethyl-2,3,4,6,7,8,9-heptasila-1,5-diarsatricyclo[3.3.1.0^{3,7}]-nonane (4): To a suspension of "Na_xAs/K_xAs" [prepared from Na (1.71 g, 74.4 mmol), K (2.18 g, 55.8 mmol) and As (9.76 g, 130.25 mmol)] in dme (500 mL) was added a solution of **2** (15.0 g, 32.56 mmol) in dme (70 mL) over a period of 1 h. The reaction mixture was then submitted to the same procedure as described above. Crystallization from heptane at –30 °C gave **4** (1.7 g, 5%) as colourless crystals. $C_{12}H_{36}As_2Si_7$ (526.88): calcd. C 27.36, H 6.89; found C 28.05, H 7.08.

Sodium Hexamethyl-2,4,6,7-tetrasila-1-phosphanido-3,5-diphosphabicyclo[3.2.1]octane (5): To a solution of **1** (12.69 g, 39.2 mmol) in dme (150 mL) was added dropwise a suspension of "Na_xP/K_xP" [prepared from Na (1.53 g, 66.73 mmol), K (3.48 g, 88.97 mmol) and white phosphorus P_4 (3.30 g, 106.5 mmol] in dme (300 mL)

Table 3. Crystal data and structure refinement for compounds **3**, **4**, **5** and **6**.

	3	**4**	**5**	**6**
Formula	$C_{10}H_{30}As_2Si_5$	$C_{12}H_{36}As_2Si_7$	$C_{18}H_{50}NaO_4P_3Si_5$	$C_{13}H_{39}P_3Si_6$
Formula weight	440.62	526.88	586.93	456.89
T [K]	293(2)	98(2)	223(2)	100(2)
Wavelength [Å]	0.71073	0.71073	0.71073	0.71073
Crystal system	monoclinic	tetragonal	orthorhombic	monoclinic
Space group	$P2_1/n$	I4(1)/a	Pca2(1)	$P2_1/c$
a [Å]	12.906(3)	33.100(6)	21.554(4)	9.6779(19)
b [Å]	22.413(5)	33.100(6)	10.747(2)	26.177(5)
c [Å]	14.551(3)	9.379(2)	30.410(6)	11.028(2)
α [°]	90	90	90	90
β [°]	96.39(3)	90	90	108.02(3)
γ [°]	90	90	90	90
V [Å^3]	4183.0(15)	10276(3)	7044(2)	2656.9(9)
Z	4	16	4	4
$\rho_{calcd.}$ [g cm^{-3}]	1.399	1.362	1.106	1.142
Absorption coefficient [mm^{-1}]	3.466	2.923	0.371	0.491
$F(000)$	1808	4352	2524	984
θ range [°]	$1.68 < \theta < 26.30$	$2.57 < \theta < 25.00$	$1.89 < \theta < 24.71$	$2.09 < \theta < 26.34$
h, k, l indices range	$-16 < h < 16$	$0 < h < 39$	$-25 < h < 15$	$-12 < h < 12$
	$-27 < k < 27$	$-2 < k < 39$	$-12 < k < 12$	$32 < k < 32$
	$-17 < l < 18$	$-2 < l < 11$	$-35 < l < 33$	$-13 < l < 13$
Reflections collected/unique	32221/8449	6461/4525	33203/11690	20473/5392
Completeness to θ = 28.35° [%]	99.7	99.9	99.9	99.7
Absorption correction	SADABS	None	SADABS	SADABS
Refinement method	Full-matrix least-squares on F^2	Full-matrix least-squares on F^2	Full-matrix least-squares on F^2	Full-matrix least-squares on F^2
Data/restraints/parameters	8449/0/327	4525/0/202	11690/1/587	5392/0/212
Goodness-of-fit on F^2	1.052	1.020	0.968	1.138
Final R indices	R_1 = 0.0295	R_1 = 0.0524	R_1 = 0.0584	R_1 = 0.0550
$[I > 2\sigma(I)]$	wR_2 = 0.0702	wR_2 = 0.1170	wR_2 = 0.1045	wR_2 = 0.1360
R indices (all data)	R_1 = 0.0372	R_1 = 0.0746	R_1 = 0.1091	R_1 = 0.0644
	wR_2 = 0.0730	wR_2 = 0.1285	wR_2 = 0.1218	wR_2 = 0.1416
Largest diff. peak/hole [e Å^{-3}]	0.956/–0.313	0.928/–0.493	0.289/–0.176	0.809/–0.536

heated at reflux. After heating for 24 h, a considerable quantity of unreacted **1** was detected by ^{29}Si NMR spectroscopy, even after treatment in an ultrasonic bath. Therefore, the suspension of "Na_xP/K_xP" and the salts were removed by decantation, and a suspension of freshly prepared "Na_xP/K_xP" (from 3.3 g of white phosphorus) was added dropwise to the solution heated at reflux. The reaction mixture was heated at reflux for another 40 h and separated from the salts by filtration. The solvent was removed by evaporation in vacuo and replaced by pentane. The insoluble residue was dissolved in hexane/dme (1:1). At –30 °C, **5** (4.9 g, 23%) was obtained as colourless crystals. $C_{18}H_{50}NaO_4P_3Si_5$ (586.93): calcd. C 36.83, H 8.59; found C 35.74, H 7.92.

Decamethyl-3-trimethylsilyl-1,3,5-triphospha-2,4,6,7-tetrasilabicyclo[3.2.1]octane (6): To a solution of **5** (2.70 g, 4.6 mmol) in pentane/dme (1:1) at –80 °C was added dropwise chlorotrimethylsilane (0.5 g, 4.6 mmol). The reaction mixture was allowed to reach r.t., and the solvents are removed completely by evaporation in vacuo. *n*-Pentane was added, and the solid precipitates were separated by decantation. At –30 °C, **6** (1.2 g, 57%) was obtained as colourless crystals. $C_{13}H_{39}P_3Si_6$ (456.89): calcd. C 34.17, H 8.60; found C 33.52, H 8.41.

X-Ray Crystal Structure Analysis: Crystals were mounted onto the tip of a glass fibre, and the data collection was performed with a BRUKER-AXS SMART APEX CCD diffractometer for compounds **3**, **5** and **6**, and a STOE four-circle diffractometer for **4**. Graphite-monochromated Mo-K_α radiation (71.073 pm) was used for the measurements. Crystal data and details of the structure refinement are summarized in Table 3. The data were reduced to F^2_o and corrected for absorption effects with SAINT[16] and SADABS.[17] The structures were solved by direct methods and refined by full-matrix least-squares method (SHELXL97).[18] All non-hydrogen atoms were refined with anisotropic displacement parameters. All hydrogen atoms were located in calculated positions to correspond to standard bond lengths and angles.

CCDC-637289 (for **3**), -637287 (for **4**), -637288 (for **5**) and -637290 (for **6**) contain the supplementary crystallographic data for this paper. These data can be obtained free of charge from The Cambridge Crystallographic Data Centre via www.ccdc.cam.ac.uk/data_request/cif.

Quantum Chemical Calculations: All considered geometries were optimized at the B3LYP/6-31G* level by using the Gaussian 03 software package.[19] The conformers with the lowest energy were considered in the discussion with their atomic charges as defined by Mullican.[20]

Acknowledgments

The authors thank the Fond zur Förderung der wissenschaftlichen Forschung, FWF, for financial support (project P 15366-NO3).

[1] For a review on polycyclic phosphanes, see for instance: M. Baudler, K. Glinka, *Chem. Rev.* **1993**, *93*, 1623; for polycyclic silanes, see: E. Hengge, R. Janoschek, *Chem. Rev.* **1995**, *95*, 1495; A. Sekiguchi, H. Sakurai, *Adv. Organomet. Chem.* **1995**, *37*, 1.
[2] See, for instance: M. Driess, A. D. Fanta, D. Powell, R. West, *Angew. Chem.* **1989**, *101*, 1087; *Angew. Chem. Int. Ed. Engl.* **1989**, *28*, 1038.
[3] U. Winkler, M. Schieck, H. Pritzkow, M. Driess, I. Hyla-Kryspin, H. Lange, R. Gleiter, *Chem. Eur. J.* **1997**, *3*, 874.
[4] G. M. Kollegger, U. Katzenbeisser, K. Hassler, C. Krüger, D. Brauer, R. Gielen, *J. Organomet. Chem.* **1997**, *543*, 103.
[5] G. M. Kollegger, H. Siegl, K. Hassler, K. Gruber, *Organometallics* **1996**, *15*, 4337.
[6] M. Driess, M. Reisgys, H. Pritzkow, *Z. Anorg. Allg. Chem.* **1998**, *624*, 1886.
[7] See, for instance: K. Tamao, A. Kawachi, *Angew. Chem. Int. Ed. Engl.* **1995**, *34*, 818; A. Kawachi, K. Tamao, *Bull. Chem. Soc. Jpn.* **1997**, *70*, 945.
[8] N. N. Greenwood, A. Earnshaw, *Chemistry of the Elements*, Pergamon Press, Oxford, **1985**.
[9] M. Ruck, D. Hoppe, B. Wahl, P. Simon, Y. Wang, G. Seifert, *Angew. Chem.* **2005**, *117*, 7788.
[10] J. Bruckmann, C. Krüger, *Acta Crystallogr., Sect. C* **1995**, *51*, 1152.
[11] U. Englich, K. Hassler, K. Ruhland-Senge, F. Uhlig, *Inorg. Chem.* **1998**, *37*, 3532.
[12] B. M. Gimarc, J. J. Ott, *J. Am. Chem. Soc.* **1983**, *105*, 1979.
[13] The relative energy of the [3.2.1] isomer with a Si_6 boat conformation is 7.6 kJ mol^{-1}.
[14] See, for instance: N. Schulze, G. Roewer in *Organosilicon Chemistry IV – From Molecules to Materials* (Eds.: N. Auner, J. Weis), Wiley-VCH, Weinheim, **2000**.
[15] G. Becker, G. Gutekunst, H. J. Wessely, *Z. Anorg. Allg. Chem.* **1980**, *462*, 113.
[16] *SAINTPLUS: Software Reference Manual*, Version 6.45, Bruker-AXS, Madison, WOI, **1997**–**2003**.
[17] R. H. Blessing, *Acta Crystallogr., Sect. A* **1995**, *51*, 33; *SADABS*, Version 2.1, Bruker-AXS, **1998**.
[18] G. M. Sheldrick, *SHELXL97: Programs for Crystal Structure Analysis (Release 97–2)*, University of Göttingen, Göttingen, Germany **1998**.
[19] M. J. Frisch, G. W. Trucks, H. B. Schlegel, G. E. Scuseria, M. A. Robb, J. R. Cheeseman, J. A. Montgomery Jr, T. Vreven, K. N. Kudin, J. C. Burant, J. M. Millam, S. S. Iyengar, J. Tomasi, V. Barone, B. Mennucci, M. Cossi, G. Scalmani, N. Rega, G. A. Petersson, H. Nakatsuji, M. Hada, M. Ehara, K. Toyota, R. Fukuda, J. Hasegawa, M. Ishida, T. Nakajima, Y. Honda, O. Kitao, H. Nakai, M. Klene, X. Li, J. E. Knox, H. P. Hratchian, J. B. Cross, C. Adamo, J. Jaramillo, R. Gomperts, R. E. Stratmann, O. Yazyev, A. J. Austin, R. Cammi, C. Pomelli, J. W. Ochterski, P. Y. Ayala, K. Morokuma, G. A. Voth, P. Salvador, J. J. Dannenberg, V. G. Zakrzewski, S. Dapprich, A. D. Daniels, M. C. Strain, O. Farkas, D. K. Malick, A. D. Rabuck, K. Raghavachari, J. B. Foresman, J. V. Ortiz, Q. Cui, A. G. Baboul, S. Clifford, J. Cioslowski, B. B. Stefanov, G. Liu, A. Liashenko, P. Piskorz, I. Komaromi, R. L. Martin, D. J. Fox, T. Keith, M. A. Al-Laham, C. Y. Peng, A. Nanayakkara, M. Challacombe, P. M. W. Gill, B. Johnson, W. Chen, M. W. Wong, C. Gonzalez, J. A. Pople, *Gaussian 03*, Revision B.03, Gaussian, Inc., Pittsburgh, PA, **2003**.
[20] R. S. Mulliken, *J. Chem. Phys.* **1962**, *36*, 3428.

Received: April 17, 2007
Published Online: July 6, 2007

